

Residual Overfit Method of Exploration

James McInerney

Netflix

JMCINERNEY@NETFLIX.COM

Nathan Kallus

Cornell University & Netflix

KALLUS@CORNELL.EDU

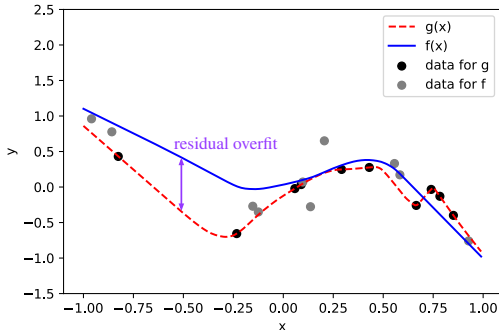
Abstract

Exploration is a crucial aspect of bandit and reinforcement learning algorithms. The uncertainty quantification necessary for exploration often comes from either closed-form expressions based on simple models or resampling and posterior approximations that are computationally intensive. We propose instead an approximate exploration methodology based on fitting only two point estimates, one tuned and one overfit. The approach, which we term the residual overfit method of exploration (ROME), drives exploration towards actions where the overfit model exhibits the most overfitting compared to the tuned model. The intuition is that overfitting occurs the most at actions and contexts with insufficient data to form accurate predictions of the reward. We justify this intuition formally from both a frequentist and a Bayesian information theoretic perspective. The result is a method that generalizes to a wide variety of models and avoids the computational overhead of resampling or posterior approximations. We compare ROME against a set of established contextual bandit methods on three datasets and find it to be one of the best performing.

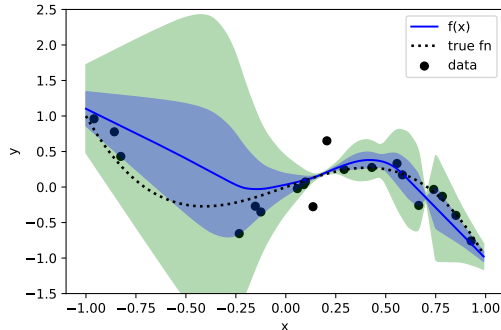
1. Introduction

The use of machine learning in interactive environments such as recommender systems [14, 18, 26] and display ads [6, 11, 15] motivates the study of how to balance taking high value actions (exploitation) with gathering diverse data to learn better models (exploration). The framework of contextual multi-armed bandits, and its extension to reinforcement learning in dynamic environments, provides guidance for addressing this important task [25]. Generally, efficient algorithms tackle the trade-off by encouraging actions with high model uncertainty, either by adding an explicit bonus for uncertainty as in upper confidence bound (UCB) algorithms [13] or by sampling from the posterior distribution over the parameters to promote uncertain actions as in Thompson sampling [6]. In either case, some quantification of uncertainty is needed.

There are several challenges to uncertainty quantification for both UCB and Thompson-sampling algorithms. With the exception of simple models like linear and/or conjugate priors, either the sampling or posterior distributions are not analytically known, and instead approximation methods are needed, such as bootstrapping, Markov chain Monte Carlo (MCMC), or variational inference (VI) [2]. Both bootstrapping and MCMC are computationally intensive and the latter requires diagnostics to assess convergence. VI is scalable but tends to require a specialized algorithm for each class of model to be effective and has the property of underestimating posterior variance due to its objective being an expectation with respect to the approximating distribution [17].



(a) Example of fitting regularized model f (blue solid line) and overfit model g (red dashed line) to toy data. The absolute difference between the two functions at any x is the residual overfit. To ensure independence between the fits, they are made on an equal-sized random split of the 20 observations.



(b) Using the same data and fits as Figure 1a, the f function is annotated with the residual overfit (inner blue shaded area) and 2.58 times the residual overfit representing an approximate 99% confidence interval (outer green shaded area). The mean of the true data generating distribution is plotted in black.

Against this background, our motivation is to develop an effective methodology for exploration that is scalable and adaptable to a wide range of models. Crucially, we seek a method of uncertainty quantification that applies to complex predictive models that may be biased. Bias is introduced because the best estimators in terms of mean-squared error use tools to prevent overfitting, such as L1/L2 regularization, bagging [3], dropout [1], early stopping [4, 20], and the like. While improving prediction, these make uncertainty quantification more difficult as the uncertainty consists of more than just variance. We show how fitting one additional model without these tools, i.e., formulating an overfit model of the data, and combining its predictions with those of the tuned estimator enables approximate uncertainty quantification. We formalize this as the *residual overfit* and we use it to drive exploration in what we call the residual overfit method of exploration (ROME).

From a frequentist perspective, the residual overfit provides an upper approximation of pointwise uncertainty. From a Bayesian information theoretical perspective, the residual overfit provides an upper approximation of the information gain from exploring at any one new point. These two perspectives suggest it is a possible approximation for driving exploration. To explore this in practice, we consider a bandit experimental setup and compare both UCB and Thompson sampling algorithms based on ROME to benchmark methods that either use resampling to tackle complex models or use exact uncertainty quantification for simple models. Across our experiments, we find ROME performs competitively, often getting the best performance, despite its simplicity and tractability. Together, our results suggest ROME is a good option for driving exploration in practical settings with complex predictive models.

2. The Residual Overfit

Definitions Given a design x_1, \dots, x_n , we consider data consisting of noisy observations of a function h , $y_i = h(x_i) + \epsilon_i$, where ϵ_i has mean zero and variance $\sigma^2(x_i)$ and is independent

of ϵ_j for $j \neq i$. Let $\mathcal{D} = (x_1, y_1, \dots, x_n, y_n)$ represent the observed data. Considering the design fixed, the randomness of \mathcal{D} reduces to the randomness of $\epsilon_1, \dots, \epsilon_n$. The design may also be random and all the conclusions would still follow since they hold for any one design. Let f and g be estimators for the unknown function h based on the training data \mathcal{D} . Function f is generally understood to be trained for estimation, i.e., for the lowest mean squared error (MSE). Function g is trained for unbiasedness, i.e., it satisfies the constraint $\mathbb{E}[g(x)] = h(x)$ for any x , where expectations are taken with respect to the training data, that is, with respect to the randomness of $\epsilon_1, \dots, \epsilon_n$. We define the **residual overfit** at x as,

$$s(x) = |f(x) - g(x)|. \quad (1)$$

Proposition 1 *When f and g are independent, the expected squared residual overfit at x is equal to the mean squared error of f plus the variance of g ,*

$$\mathbb{E}[s(x)^2] = \text{MSE}[f(x)] + \text{Var}[g(x)], \quad (2)$$

where $\text{MSE}[f(x)] = \mathbb{E}[(f(x) - h(x))^2]$. Recall \mathbb{E} and Var are taken with respect to the training data. Note x is a fixed input and is not random.

Proof We have

$$\mathbb{E}[s(x)^2] = \mathbb{E}[(f(x) - h(x)) - (g(x) - h(x))]^2 \quad (3)$$

$$= \text{MSE}[f(x)] + \text{MSE}[g(x)] + \text{Cov}(f(x) - h(x), g(x) - h(x)) \quad (4)$$

$$= \text{MSE}[f(x)] + \text{Var}[g(x)], \quad (5)$$

where the last equality is by the unbiasedness of g and the independence of f and g . ■

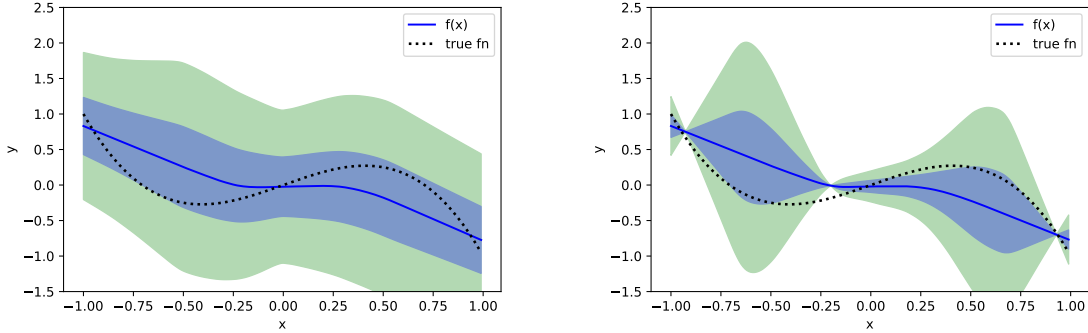
The estimators f and g can be made independent by training on two disjoint random splits of the data.

Why not fit a model to the prediction error of f instead? An appealing alternative in studying the error of f may be to directly fit a predictive model of the squared error of f . This, however, involves *both* the estimation error and the noise. Namely, fix x_0 and consider $y_0 = h(x_0) + \epsilon_0$; then predicting the error of f at x_0 would estimate $\mathbb{E}[(f(x_0) - y_0)^2] = (f(x_0) - h(x_0))^2 + \sigma^2(x_0)$. Taking expectations over the data as well yields $\mathbb{E}[(f(x_0) - y_0)^2] = \text{MSE}[f(x_0)] + \sigma^2(x_0)$. Thus, at best, a model for the prediction error of f would involve the irreducible variance $\sigma^2(x_0)$, which does not vanish. Therefore, this may not well reflect the estimation error of f . This is known as the white noise problem in reinforcement learning [23]. In contrast, the expected squared residual overfit only involves estimation errors. In addition, if the data is heteroskedastic, then $\sigma^2(x)$ will vary across x even under no model uncertainty and will incorrectly bias exploration.

See Figure 2 for a visual comparison of the two approaches.

3. Residual Overfit Method of Exploration (ROME)

The properties of the squared residual overfit in Eq. 2 are suggestive of the variance term in standard approaches for exploration-exploitation. Consider the discrete action set $a \in \mathcal{A}$



(a) Shaded areas show the output of a model trained to predict the RMSE of f and 2.58 times the RMSE of f . (b) Shaded areas show the residual overfit and 2.58 times the residual overfit.

Figure 2: Using root mean squared error (RMSE) as the training target results in smoother interpolation of error bars but does not encourage exploration toward regions without support. In this example, 100 data points are generated at each point $x \in \{-1, -\frac{1}{2}, 0, \frac{1}{2}, 1\}$. In Figure 2a, the predicted uncertainty remains constant even though there is higher certainty at the observed inputs. In Figure 2b, the highest regions of predicted uncertainty fall outside the observed inputs. Data are omitted for legibility.

with context $x \in \mathcal{X}$ comprising continuous and/or discrete features. Before each interaction with the environment, the bandit observes a context x and must score each action a . The action with the maximum score is taken greedily. The residual overfit may be applied to this setting using the following scores,

$$\hat{y}_a = f(a, x) + \alpha |f(a, x) - g(a, x)| \quad (\text{UCB}) \quad (6)$$

$$\hat{y}_a \sim p(f(a, x), (f(a, x) - g(a, x))^2) \quad (\text{Thompson sampling}) \quad (7)$$

for some exploration hyperparameter α . Exploration is guided towards actions where either the reward or error of f is high, or the variance of g is high. This approach is called the *residual overfit method of exploration* (ROME). Note that ROME uses a single sample (i.e. a dataset) Monte Carlo estimate of the expectation presented in Eq. 2. If pure exploration is required, the $f(a, x)$ value outside of the residual overfit terms in Eq. 6 and Eq. 7 may be replaced with 0.

3.1 Exponential Family Moment Matching

We consider how to apply the method to exponential families. Many distributions of interest belong to the exponential family, e.g., univariate or multivariate Gaussian, Bernoulli, multinomial, Poisson [27]. In deep neural networks and decision trees, the last layer typically includes a member of the exponential family that induces a loss with respect to the observations and latent representation.

Exponential family distributions over random variable y take the form,

$$p(y | \eta) \propto \exp \left\{ t(y)^\top \eta \right\}, \quad (8)$$

with natural parameter η and sufficient statistics $t(y)$.

Distributions in the exponential family have the property that the distribution that minimizes the KL divergence from the target distribution with a given mean and variance is obtained by matching moments. Here, we use $(f(x), (f(x) - g(x))^2)$ as the mean and variance.

3.1.1 BINARY OUTCOMES

Use Beta(a, b) distribution to model the probability of binary outcomes. If f has been trained to minimize Bernoulli (logistic) loss then its output is a suitable candidate as the mean of the Beta distribution, given its conjugate relationship with the Bernoulli (i.e. updating a Beta prior with Bernoulli evidence with Bayes' rule yields another Beta distribution). We can calculate the Beta pseudo-counts (a, b) by matching the mean and variance,

$$\begin{aligned}\mathbb{E}[p_f] &= \frac{a}{a+b} := f(x) \\ \text{Var}[p_f] &= \frac{ab}{(a+b)^2(a+b+1)} := (f(x) - g(x))^2\end{aligned}\tag{9}$$

$$\begin{aligned}\implies a &= f(x) \left| \frac{f(x)(1-f(x))}{(f(x)-g(x))^2} - 1 \right| \\ b &= (1-f(x)) \left| \frac{f(x)(1-f(x))}{(f(x)-g(x))^2} - 1 \right|\end{aligned}\tag{10}$$

If we interpret the output of f as the Bernoulli probability p_f of binary outcome y with Beta prior, then the posterior parameters are equivalent to,

$$\begin{aligned}a &= \mathbb{E}[p_f] \left| \frac{\text{Var}_{p_f}[Y]}{\text{Var}[p_f]} - 1 \right| \\ b &= (1 - \mathbb{E}[p_f]) \left| \frac{\text{Var}_{p_f}[Y]}{\text{Var}[p_f]} - 1 \right|.\end{aligned}\tag{11}$$

4. Bayesian Information Theoretical Perspective

The analysis so far has required the errors of f and g to be independent, necessitating random data splits. It is not ideal to split the data because it will lead to worse estimates, especially with small data sizes. Is it possible to analyze ROME when f and g are not trained on different splits of the training data? To address this question and provide a broader perspective on the residual overfit, we now consider it in the setting of Bayesian information theory.

There are various information theoretic criteria for choosing the next action with Bayesian inference. A prominent class of methods maximizes the information gain for the parameters θ from unknown response y given dataset \mathcal{D} ,

$$\begin{aligned}x^* &= \arg_x \max I_x[\theta, y | \mathcal{D}] \\ \text{where } I_x[\theta, y | \mathcal{D}] &= H[\theta | \mathcal{D}] - H_x[\theta | \mathcal{D}, y],\end{aligned}\tag{12}$$

where the subscript x is used to indicate an arbitrary fixed query point. Eq. 12 is equivalent to maximizing the decrease in posterior entropy after the new observation [17]. Due to symmetry of information gain, Eq. 12 can be expressed in terms of entropy of the predicted target, avoiding unnecessary posterior updates [10, 16],

$$I_x[\theta, y | \mathcal{D}] = H_x[y | \mathcal{D}] - H_x[y | \mathcal{D}, \theta] \quad (13)$$

The model appears twice in Eq. 13: in the first term with parameters marginalized out and in the second term with posterior averaged entropy. Due to this, the approach is unreliable when the predictive uncertainty of y is underestimated, since it determines both the entropy and conditional entropy. In fact, in the limiting case of a point estimate for the posterior, such as the maximum *a posteriori* (MAP) estimate, the information gain is zero across all x .

Our diagnosis of the problem of approximating information gain is that it is misleading to use the predictive entropy of y under the *typical* parameter in the first term of Eq. 13 (e.g. using variational inference or MAP). The peril is that the uncertainty of some actions is underestimated and leads to their elimination in an interactive setting, a type II error in identifying actions requiring exploration. In contrast, overestimating uncertainty (type I error) leads to self-correction over time as more samples are gathered. To reflect this explorative asymmetry, we consider the *lowest upper bound* of the predictive entropy induced by an approximating distribution q . To formalize this notion, for any q , add a non-negative slack (recall, any KL divergence is non-negative) to the information gain,

$$\begin{aligned} I_x[\theta, y | \mathcal{D}] &\leq \hat{I}_{q,x}[\theta, y | \mathcal{D}] \\ &:= I_x[\theta, y | \mathcal{D}] + \text{KL}[p(y | \mathcal{D}, x) || q(y | x)] \\ &= -\mathbb{E}_{p(y | \mathcal{D}, x)}[\log q(y | x)] - H_{\mathcal{D}, x}[y | \theta], \end{aligned} \quad (14)$$

then look for q that minimizes $\hat{I}_{q,x}[y, \theta | \mathcal{D}]$ under the empirical average of $x \sim \mathcal{D}$. This is equivalent to minimizing $\mathbb{E}_{x \sim \mathcal{D}}[\text{KL}[p(y | \mathcal{D}, x) || q(y | x)]]$ which goes to zero as q gets closer to the marginal predictive probability. Eq. 14 can be rewritten as the KL divergence between the prediction of the model and the approximation,

$$\hat{I}_{q,x}[\theta, y | \mathcal{D}] = \mathbb{E}_{p(\theta | \mathcal{D})} \text{KL}[p(y | \theta, x) || q(y | x)]. \quad (15)$$

Eq. 15 may be estimated as follows. The approximation for the distribution of the outer expectation must be close to the true posterior $p(\theta | \mathcal{D})$. Hence, it is amenable to established methods for approximate Bayesian inference such as MCMC, variational inference, or MAP. As discussed before, the empirical q approximation for the RHS of the KL divergence in Eq. 15 minimizes $\mathbb{E}_{x \sim \mathcal{D}}[\text{KL}[p(y | \mathcal{D}, x) || q(y | x)]]$. When $p(y | \mathcal{D}, x)$ is the true data generating distribution then q is the maximum likelihood solution.

For a univariate Gaussian distribution on y , Eq. 15 reduces to a closed-form expression,

$$\hat{I}_{q,x}[\theta, y | \mathcal{D}] = \frac{1}{2\sigma^2} (f(x) - g(x))^2 + \text{constant}, \quad (16)$$

where $f(x)$ is the mean prediction of a MAP inferred model, $g(x)$ is the mean prediction of the q model, and σ^2 is the irreducible variance. This recovers ROME in the deterministic exploration setting when $\sigma^2 = \frac{1}{2}$.

Eq. 15 extends to other observation likelihoods, e.g., the Bernoulli observation likelihood yields,

$$\hat{\mathbb{I}}_{q,x}[\theta, y | \mathcal{D}] = g(x) \log \frac{g(x)}{f(x)} + (1 - g(x)) \log \frac{1 - g(x)}{1 - f(x)}, \quad (17)$$

where $f(x)$ and $g(x)$ are the MAP and q model probabilities of success, respectively. Poisson observation likelihood results in,

$$\hat{\mathbb{I}}_{q,x}[\theta, y | \mathcal{D}] = g(x) \log \frac{g(x)}{f(x)} + f(x) - g(x), \quad (18)$$

where $f(x)$ is the mean predicted rate of the MAP model and $g(x)$ is the mean predicted rate of the q model.

4.1 Practicality of ROME

When deploying a model in practice, it is standard procedure to perform a hyperparameter search to find the model architecture and training settings that perform best on held-out validation data. In this way, an overfit model, which we call g , is a by-product in the search for the best f . There are two main benefits to this observation. First, in this setting, ROME avoids additional training time. Second, there is low marginal engineering cost for deploying g , since it was at one point a candidate for f , so likely has much in common with f such as features, targets, training algorithm, and deployment pipeline.

What procedure should be used to select g out of a candidate set of models? While it is likely advantageous to combine more than one overfit model, perhaps by cycling through them by iteration to encourage diversity, we have focused here on the case where there is a single g for generality and ease of exposition. Theory suggests that g should be selected to give the lowest variance unbiased estimate of the reward.

5. Related Work

There are various scalable algorithms that combine uncertainty quantification and model expressibility. Stochastic gradient Langevin dynamics (SGLD) [28] adds noise to stochastic gradients in order to sample from a posterior distribution under appropriate conditions for the optimization surface and step size. SGLD applies to gradient-based models and, in a bandit setting, requires taking multiple gradient steps at prediction time to avoid correlated samples. Variational dropout [8, 12] adapts the method of dropout regularization to perform variational approximation. It applies to deep neural networks and, since it is based on VI, underestimates posterior variance [17]. Bootstrapped Thompson sampling [19] treats a set of models trained on bootstrap resamples of a dataset as samples of the parameters over which Thompson sampling may be applied. It can be used with the widest range of models but requires either resampling then training a model on each step or training multiple models from resamples in batch mode. If the rewards are sparse then a large number of resamples are required in batch mode.

In practice, methods that perform shallow exploration are popular due to the ease with which they equip existing tuned models with exploration. Epsilon-greedy, Boltzmann

exploration [5], and last-layer variance [24] admit highly expressive models but ignore the uncertainty of most or all of the parameters [21]. This inflexibility may be compensated in some cases by an accurate tuning and decay of the exploration rate or temperature.

6. Empirical Evaluation

In the empirical evaluation we compare ROME against several benchmarks and find that it performs competitively against both shallow and deep exploration methods.

Methods The following methods are compared in the empirical evaluation,

- **Rome-TS**: ROME with Thompson sampling. Sample score from $\text{Beta}(a, b)$ with pseudo-counts given by Eq. 10.
- **Rome-UCB**: ROME with upper confidence bound. Upper confidence bound score of $\text{Beta}(a, b)$ with pseudo-counts given by Eq. 10.
- **LinUCB**: contextual bandits with linear payoffs using the upper confidence bound [7].
- **Epsilon greedy**: pick the action with the highest predicted reward with probability $(1 - \epsilon)$ and a uniform random action with ϵ probability on each step.
- **Bootstrap-TS**: bootstrap the replay buffer and train M models on each of the M replications of the data [19]. Thompson sampling is implemented by sampling one model uniformly each step and using its predicted rewards greedily to pick the action.
- **Uniform random**: pick the action uniform randomly on each step. Equivalent to epsilon greedy with $\epsilon = 1$.

In the experiments, Bootstrap-TS uses $M = 20$ replications, making training 20 times as computationally intensive as epsilon greedy and 10 times as computationally intensive as ROME. For the UCB methods, the weighting for the upper bound is set to $\alpha = 1$ and $\epsilon = 0.1$ in epsilon greedy.

With the exception of epsilon greedy and uniform random, all methods are controlled with the same implementation settings using,

- a random forrest reward classifier model with the default settings from the `scikit-learn` package¹ which uses an ensemble of 10 decision trees.
- A constant explore rate of 0.01 to mimic a small number of organic observations arriving outside of the bandit channel [22].
- The model is retrained every 100 iterations. In real-world settings it is usually infeasible to retrain after every interaction, necessitating batched interactions.

1. version 0.21.1 <https://scikit-learn.org/0.21/>

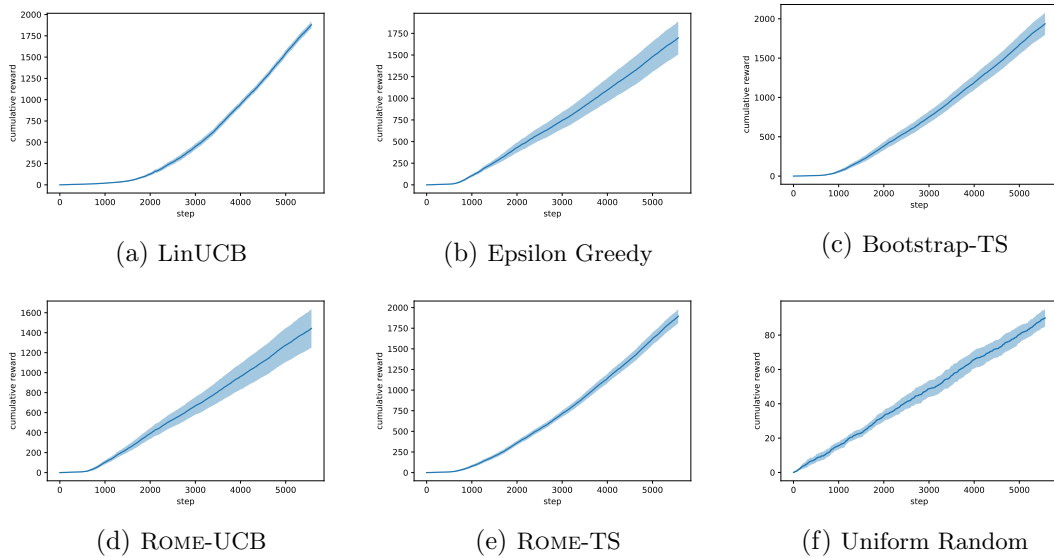


Figure 3: Cumulative reward curves for the Bach Chorales dataset.

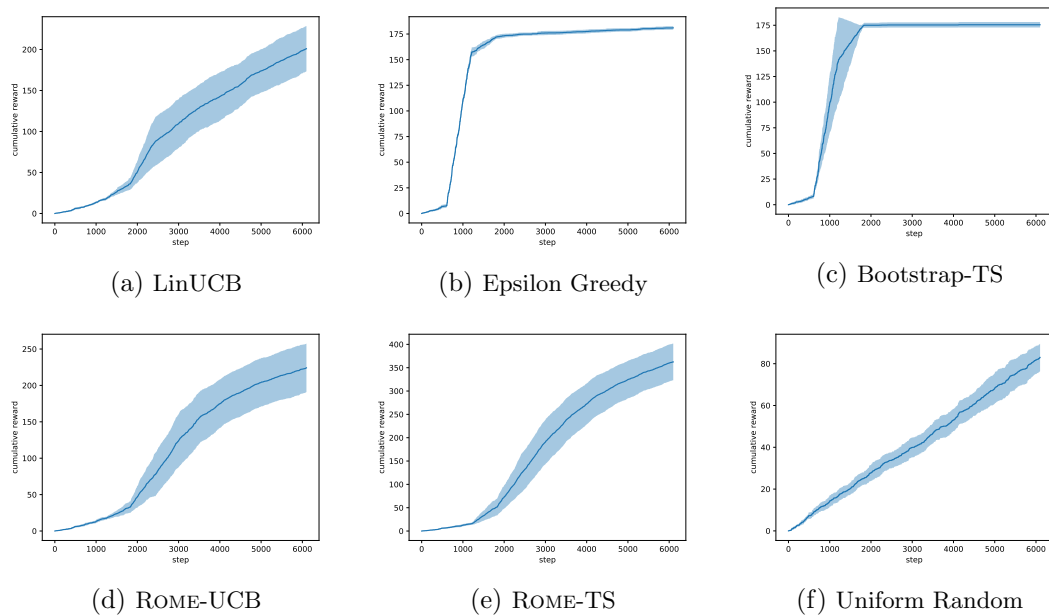


Figure 4: Cumulative reward curves for the MovieLens-deleting dataset.

Table 1: Average regret with 95% confidence interval over 10 replications. Top performing method for each dataset in bold.

Method	Covertypes (7 classes)	Bach Chorales (65 classes)	MovieLens-depleting (3,600 classes)
LinUCB	0.415 ± 0.003	0.664 ± 0.007	0.967 ± 0.005
Epsilon Greedy	0.403 ± 0.005	0.711 ± 0.051	0.970 ± 0.000
Bootstrap-TS	0.390 ± 0.003	0.668 ± 0.028	0.971 ± 0.000
ROME-UCB	0.422 ± 0.004	0.718 ± 0.035	0.963 ± 0.005
ROME-TS	0.524 ± 0.004	0.657 ± 0.012	0.941 ± 0.006
Uniform Random	0.859 ± 0.004	0.985 ± 0.001	0.986 ± 0.001

Datasets Evaluating explore-exploit performance requires setting up an interactive environment to assess the impact of acquired data on subsequent performance. We consider three classification datasets, and in each case, partial feedback is simulated by the environment providing a reward of 1 if the action corresponding true class is chosen and 0 otherwise. The instances are held in an arbitrary random order across 10 repetitions of the experiments. Actions are performed uniformly at random until every action has been observed at least once. The random seed for the methods and initial exploration varies across repetitions. The following datasets are studied,

- **Covertypes:** data comprises 7 classes of forest cover type predicted from 54 attributes over 581,012 instances.²
- **Bach Chorales:** Bach chorale harmony dataset with 17 features to predict 65 classes of harmonic structure in 5,665 examples.³
- **MovieLens-depleting:** a matrix of 100,000 interactions between 610 users and 7,200 items [9]. To replicate the cold start task recommender systems face when introducing new items, we split the items randomly into two equal-sized groups: existing items and cold start items. The bandit has access to all the historical user and existing item interactions but the interactions between users and cold start items receives only partial feedback. In each step of the experiment, the bandit chooses which cold start item to recommend to a user based on the observed interaction and context history. The bandit makes 10 passes through the dataset. To replicate the depleting effect of consuming items, the same cold start item and user may give a reward of 1 no more than once, and subsequently 0.

Results In Table 1, we find that ROME performs well across the datasets. Bootstrap-TS performs best for small action spaces where the rewards are denser. As the number of actions grows, it becomes harder for a small number of positive examples to appear in a significant number of bootstrap samples. Across datasets, the Thompson sampling approaches (ROME-TS and Bootstrap-TS) outperformed the UCB methods. This is likely

2. <https://archive.ics.uci.edu/ml/datasets/covertypes>

3. <https://archive.ics.uci.edu/ml/datasets/Bach+Choral+Harmony>

due to the benefit of stochasticity in the batch action setting in addition to the strong empirical performance for Thompson sampling observed more generally [6].

Figure 3 shows the cumulative reward curves of the methods as a function of the number of interactions in the Bach Chorales dataset. Early on, LinUCB explores more than the other model-based approaches, and as a result, Bootstrap-TS achieves the highest cumulative reward at the end. The most challenging dataset was MovieLens-depleting, due to both the large action space (3,600 actions) and depleting rewards. For this dataset, Figure 4 illustrates how only LinUCB, ROME-TS, and ROME-UCB were able to continue discovering high value actions after 10 passes through the dataset.⁴

7. Conclusions

In this paper we developed theoretical and empirical justifications for the merits of combining a tuned and overfit model for exploration. The residual overfit method of exploration (ROME) approximately identifies actions and contexts with the highest parameter variance. The method can be applied to explore-exploit settings by adding the best regularized estimate of the reward. We provided a frequentist interpretation and a Bayesian information theoretic interpretation that shows that the residual overfit approximates an upper bound on the information gain of the parameters. Experiments comparing ROME with widely used alternatives shows that it performs well at balancing exploration and exploitation.

Acknowledgments

We thank Nikos Vlassis, Ehsan Saberian, Dawen Liang, Pannaga Shivaswamy, Maria Dimakopoulou, Yves Raimond, Darío García-García, and Justin Basilico for their insightful feedback.

References

- [1] P. Baldi and P. J. Sadowski. Understanding dropout. *Advances in neural information processing systems*, 26:2814–2822, 2013.
- [2] C. M. Bishop. Pattern recognition. *Machine learning*, 128(9), 2006.
- [3] L. Breiman. Bagging predictors. *Machine learning*, 24(2):123–140, 1996.
- [4] R. Caruana, S. Lawrence, and L. Giles. Overfitting in neural nets: Backpropagation, conjugate gradient, and early stopping. *Advances in neural information processing systems*, pages 402–408, 2001.
- [5] N. Cesa-Bianchi, C. Gentile, G. Neu, and G. Lugosi. Boltzmann exploration done right. In *Advances in neural information processing systems*, pages 6287–6296, 2017.
- [6] O. Chapelle and L. Li. An empirical evaluation of Thompson sampling. *Advances in neural information processing systems*, 24:2249–2257, 2011.

4. This holds for Uniform trivially since it depletes the popular items much slower than the other methods.

- [7] W. Chu, L. Li, L. Reyzin, and R. Schapire. Contextual bandits with linear payoff functions. In *Proceedings of the Fourteenth International Conference on Artificial Intelligence and Statistics*, pages 208–214. JMLR Workshop and Conference Proceedings, 2011.
- [8] Y. Gal and Z. Ghahramani. Dropout as a Bayesian approximation: Representing model uncertainty in deep learning. In *International conference on machine learning*, pages 1050–1059. PMLR, 2016.
- [9] F. M. Harper and J. A. Konstan. The Movielens datasets: History and context. *Acm transactions on interactive intelligent systems (TIIS)*, 5(4):1–19, 2015.
- [10] N. Houlsby, F. Huszár, Z. Ghahramani, and M. Lengyel. Bayesian active learning for classification and preference learning. *arXiv preprint arXiv:1112.5745*, 2011.
- [11] O. Jeunen, D. Mykhaylov, D. Rohde, F. Vasile, A. Gilotte, and M. Bompaire. Learning from bandit feedback: An overview of the state-of-the-art. *arXiv preprint arXiv:1909.08471*, 2019.
- [12] D. P. Kingma, T. Salimans, and M. Welling. Variational dropout and the local reparameterization trick. *Advances in neural information processing systems*, 28:2575–2583, 2015.
- [13] T. L. Lai and H. Robbins. Asymptotically efficient adaptive allocation rules. *Advances in applied mathematics*, 6(1):4–22, 1985.
- [14] L. Li, W. Chu, J. Langford, and R. E. Schapire. A contextual-bandit approach to personalized news article recommendation. In *Proceedings of the 19th international conference on World Wide Web*, pages 661–670, 2010.
- [15] W. Li, X. Wang, R. Zhang, Y. Cui, J. Mao, and R. Jin. Exploitation and exploration in a performance based contextual advertising system. In *Proceedings of the 16th ACM SIGKDD international conference on Knowledge discovery and data mining*, pages 27–36, 2010.
- [16] D. V. Lindley. On a measure of the information provided by an experiment. *The Annals of Mathematical Statistics*, pages 986–1005, 1956.
- [17] D. J. MacKay. Information-based objective functions for active data selection. *Neural computation*, 4(4):590–604, 1992.
- [18] J. McInerney, B. Lacker, S. Hansen, K. Higley, H. Bouchard, A. Gruson, and R. Mehrotra. Explore, exploit, and explain: personalizing explainable recommendations with bandits. In *Proceedings of the 12th ACM conference on recommender systems*, pages 31–39, 2018.
- [19] I. Osband, C. Blundell, A. Pritzel, and B. Van Roy. Deep exploration via bootstrapped DQN. *Advances in neural information processing systems*, 29:4026–4034, 2016.

- [20] L. Prechelt. Early stopping-but when? In *Neural networks: tricks of the trade*, pages 55–69. Springer, 1998.
- [21] C. Riquelme, G. Tucker, and J. Snoek. Deep Bayesian bandits showdown: An empirical comparison of Bayesian deep networks for Thompson sampling. *arXiv preprint arXiv:1802.09127*, 2018.
- [22] O. Sakhi, S. Bonner, D. Rohde, and F. Vasile. Blob: A probabilistic model for recommendation that combines organic and bandit signals. In *Proceedings of the 26th ACM SIGKDD international conference on knowledge discovery & data mining*, pages 783–793, 2020.
- [23] J. Schmidhuber. Formal theory of creativity, fun, and intrinsic motivation (1990–2010). *IEEE Transactions on Autonomous Mental Development*, 2(3):230–247, 2010.
- [24] J. Snoek, O. Rippel, K. Swersky, R. Kiros, N. Satish, N. Sundaram, M. Patwary, M. Prabhat, and R. Adams. Scalable bayesian optimization using deep neural networks. In *International conference on machine learning*, pages 2171–2180. PMLR, 2015.
- [25] R. S. Sutton and A. G. Barto. *Reinforcement learning: An introduction*. MIT press, 2018.
- [26] H. P. Vanchinathan, I. Nikolic, F. De Bona, and A. Krause. Explore-exploit in top-n recommender systems via Gaussian processes. In *Proceedings of the 8th ACM Conference on Recommender systems*, pages 225–232, 2014.
- [27] M. J. Wainwright and M. I. Jordan. *Graphical models, exponential families, and variational inference*. Now Publishers Inc, 2008.
- [28] M. Welling and Y. W. Teh. Bayesian learning via stochastic gradient Langevin dynamics. In *Proceedings of the 28th international conference on machine learning*, pages 681–688. Citeseer, 2011.